Journal Homepage: https://dergipark.org.tr/tr/pub/isibted

Isı Bilimi ve Tekniği Dergisi

Archive: https://tibtd.org.tr/dergi

Investigation of Flow and Heat Transfer Performance of Gyroid Structure as Porous Media

Alper Mete GENÇ [1,2] *, Ziya Haktan KARADENİZ [3]

[1] *Graduate School of Natural and Applied Sciences, Izmir Kâtip Celebi University, Izmir, Türkiye*
[2] *Bosch Thermotechnology, Manisa, Türkiye*
[3] *Energy Systems Engineering, Izmir Institute of Technology, Izmir, Türkiye*

A R T I C L E I N F O

2024, vol. 44, no.2, pp. 351-358

doi: 10.47480/isibted.1471713

Research Article
Received: 22 April 2024
Accepted: 20 August 2024

* *Corresponding Author*
e-mail: alper.m.genc@gmail.com

Keywords:
Heat exchanger
Heat transfer
TPMS
Gyroid
Porous media

ORCID Numbers in author order:
0000-0002-1290-9962
0000-0001-7850-7942

A B S T R A C T

There are active and passive methods used to improve heat transfer. One of the passive methods is utilising porous media with high heat transfer surface area. Porous media are divided into two groups: regular and irregular structures. One of the regular structures is triply periodic minimal surfaces (TPMS), which have been studied quite frequently recently. In this study, heat transfer and flow analysis of a Gyroid geometry, one of the most used TPMS in the literature, is investigated numerically considering the conjugate heat transfer conditions. A single porosity is considered (ε = 0.6), and aluminium, ceramic and PLA are selected for the heat exchanger material to examine the temperature change in the heat exchanger. To understand the different flow characteristics, Reynolds numbers are assumed to be 19.12, 95.61 and 172.09. The fluid inlet temperature is assumed to be constant at 298.15 K, and the initial temperature of the heat exchanger is assumed to be constant at 278.15 K to be consistent with the regenerative heat recovery temperature difference in ventilation standards. Nusselt numbers under different operating conditions are compared, and it is the ceramic material with low thermal diffusivity is at the highest level despite its low thermal conductivity. At the highest Reynolds number, it provided approximately 6% better heat transfer than the aluminium heat exchanger.

Gözenekli Ortam Olarak Gyroid Yapısının Akış ve Isı Transferi Performansının İncelenmesi

M A K A L E B İ L G İ S İ

Anahtar Kelimeler:
Isı değiştirici
Isı transfer
ÜYPMY
Gyroid
Gözenekli yapı

Ö Z E T

Isı transferini iyileştirmek için aktif ve pasif yöntemler kullanılmaktadır. Pasif yöntemlerden biri yüksek ısı transfer yüzey alanına sahip gözenekli ortamlardan faydalanmaktır. Gözenekli ortamlar düzenli ve düzensiz yapılar olmak üzere iki gruba ayrılır. Düzenli yapılardan biri de son zamanlarda sıkça çalışılan üçlü periyodik minimal yüzeylerdir (TPMS). Bu çalışmada, literatürde en çok kullanılan TPMS'lerden biri olan Gyroid geometrisinin ısı transferi ve akış analizi, eşlenik ısı transferi koşulları dikkate alınarak sayısal olarak incelenmiştir. Tek bir gözeneklilik (ε = 0.6) dikkate alınmış ve ısı değiştiricideki sıcaklık değişimini incelemek için ısı değiştirici malzemesi olarak alüminyum, seramik ve PLA seçilmiştir. Farklı akış karakteristiklerini anlamak için Reynolds sayılarının 19.12, 95.61 ve 172.09 olduğu varsayılmıştır. Akışkan giriş sıcaklığının 298,15 K'de sabit olduğu ve ısı değiştiricinin başlangıç sıcaklığının havalandırma standartlarındaki rejeneratif ısı geri kazanım sıcaklık farkıyla tutarlı olması için 278,15 K'de sabit olduğu varsayılmıştır. Farklı çalışma koşulları altındaki Nusselt sayıları karşılaştırılır ve düşük termal iletkenliğine rağmen düşük termal difüziviteye sahip seramik malzeme en yüksek seviyededir. En yüksek Reynolds sayısında, alüminyum ısı değiştiriciden yaklaşık %6 daha iyi ısı transferi sağlamıştır.

NOMENCLATURE

α	Thermal Diffusivity [m^2/s]	h	Heat Transfer Coefficient [W/m^2K]
a_p	Specific Area [m^2/m^3]	k	Thermal Conductivity [W/mK]
c_p	Specific Heat Capacity [J/kgK]	L	Length [m]
d_h	Hydraulic Diameter [m]	t	Time [s]
d_{hf}	Hydraulic Diameter [m]	μ	Dynamic Viscosity [Ns/m^2]
d_p	Pore Diameter [m]	D	Diameter [m]
ε	Porosity [-]	ΔP	Pressure Drop [Pa]
f	Friction factor [-]	Nu	Nusselt Number [-]
F_v^2	Pressure Exerted by the Fluid [Pa]	Re	Reynolds Number [-]
ρ	Density [kg/m^3]	V	Velocity [V]

INTRODUCTION

The advancement of technology has prompted researchers to explore various methods to enhance heat transfer effectively. Two primary approaches in this regard are active and passive methods. Active methods involve imparting additional energy to the heat-transferring fluid using external means, such as mechanical auxiliaries, rotating surfaces, mechanical mixing of flows, high or low-frequency surface vibration, flow vibration, and electrostatic fields. On the other hand, passive methods aim to improve heat transfer without additional energy input. This can be achieved through strategies such as coating heat transfer surfaces with materials of higher thermal conductivity, altering the heat transfer surface geometry, or creating intricate surface designs to increase surface area.

Increased heat transfer surface areas are commonly utilized in heat exchangers to enhance thermal efficiency. Among passive methods, the use of porous media has gained popularity due to its ability to increase heat transfer through a combination of high surface area and the formation of vortices within its complex structure. Porous media are light, compact, and can also be load-bearing materials. They find applications in diverse fields, such as aerospace engineering for evaporative cooling, electronic cooling, solar collectors, methane converters, catalytic converters, medical implantology, and heat exchangers.

Porous media can be categorized into two main types: periodic (regular) and stochastic (irregular) structures, distinguished primarily by the arrangement of pores which are shown in Figure 1 (Xu et al. 2015). Triply Periodic Minimal Surfaces (TPMS) are widely used structures among periodic porous media. TPMS consists of a combination of infinite, non-intersecting regions that repeat periodically in three main directions. These regions are qualified by having zero mean curvature (H = 0) at each point, which means that the curvature along the main curvature planes is equal. Neovius created his own structure in 1833 (Neovius, 1883), and Schwarz built up one of the most using structure, Diamond in 1865 (Schwarz, 1890). Subsequently, several other minimal surfaces, such as the Primitive and Hexagonal, were also discovered. In 1970, Schoen introduced many types of minimal surfaces, among which the Gyroid surface became particularly well-known (Schoen, 1970).

Femmer et al. (2015) found that the sheet-Diamond structure heat exchanger showed a better heat transfer performance according to the sheet-Gyroid, IWP, and Primitive geometries for a constant wall thickness (t=0.4 mm), under the laminar flow conditions (Re<15).

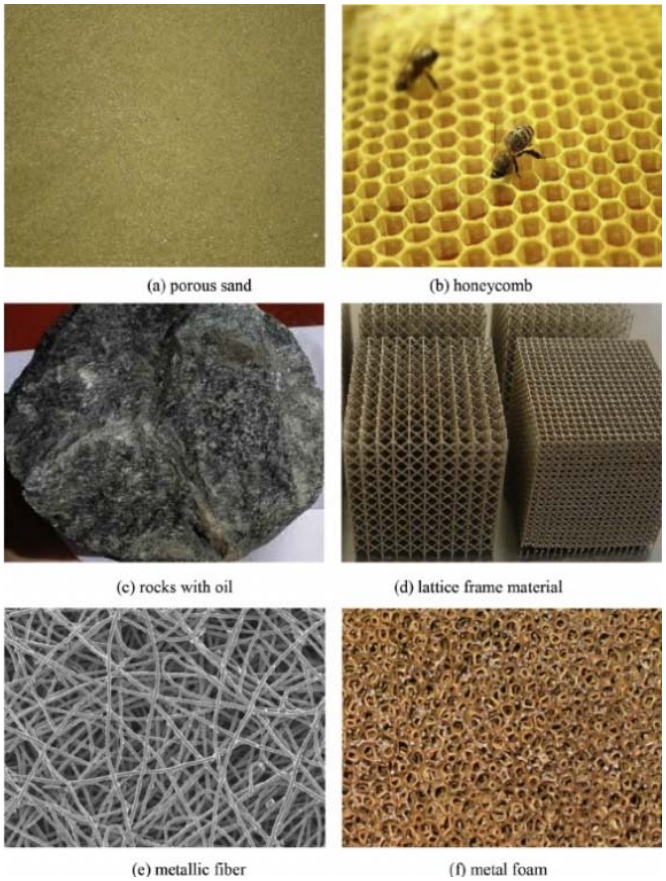

Figure 1. Different kinds of regular and irregular porous media (Xu et al. 2015)

Passos (2019) also indicated that sheet-diamond structure exhibited the best thermal performance. Iyer et al. (2022) emphasized that the sheet-Primitive geometry performed lowest heat performance, whereas the sheet-Diamond geometry had the best heat transfer performance. Reynolds (2020) found that Gyroid showed the best heat transfer performance compared to Diamond, flat plate heat exchanger and primitive for Re<2. Dharmalingam et al. (2022) presented that the TPMS heat exchangers improved heat transfer as 15–120% than a printed circuit heat exchanger for a constant pumping power. The Fischer Koch S heat exchanger increased the heat transfer performance as 23–356% at a constant pressure drop compared with the Diamond structure. Kaur and Singh (2021) numerically studied the comparison of the averaged heat transfer coefficient of the sheet-Gyroid and Primitive structures for a constant porosity and heat flux. According to the results, the sheet-Gyroid structure improved heat transfer coefficient more than the sheet-Primitive structure. Peng et al. (2019) observed that the Gyroid heat exchanger improved heat transfer rates by 7.5 times

compared to a traditional plate heat exchanger. Tang et al. (2023), focused on that heat transfer properties of TPMS geometries, distinctive TPMS structures of convective heat transfer mechanism and yield of heat distribution. Gyroid, Diamond, IWP and fins structures are evaluated. Based on this research, they conclude that the convective heat transfer coefficient of diamond 85% -207% higher, Gyroid 55%-137% higher, IWP 16%-55% higher than traditional heat transfer mechanism fins. In addition, diamond average convective heat transfer coefficient is 19.5%-37.2. % bigger than Gyroid. Reynolds et al. (2023) researched concentrates on the experimental characterization of pressure drop and heat transfer entire TPMS heat exchanger that produced via additive manufacturing. In order to observe temperature distribution in the heat exchanger, polymer has been chosen as heat exchanger material. This study focused on comparison of heat transfer and pressure drop of TPMS geometries and straight tube heat exchangers. In addition, this research Gyroid, Primitive, Diamond, F-K-S, F-K-C, IWP, Split P, F-RD, G Prime geometries are evaluated. In experimental test system, just straight tube heat exchanger and Gyroid heat exchanger are examined. After simulations and physical test results, when the pumping power is equal, Gyroid is 13% better Nusselt number than straight tube heat exchanger. Barakat and Bei Bei (2024) investigated heat transfer performance of sheet Gyroid, Diamond, SplitP and Lidinoid and five different sheet TPMS geometries which are proposed by them. According to their numerical results, TPMS2 which is proposed by authors showed better performance than sheet-Gyroid and sheet-Diamond geometries as 27.2% and 18%, respectively. Qian et al. (2024) experimentally investigated heat transfer characteristics of copper sheet- Gyroid, Primitive and Fischer- Koch S TPMS heat exchangers. Sheet Fischer-Koch S structure exhibited better heat transfer performance than sheet-Gyroid and sheet-Primitive structures. When comparing the three TPMS structures, the Fischer-Koch S structure performed 245.1% and 64.8% higher heat transfer performance than the Primitive and Gyroid structures, respectively. Alteneiji et al. (2022) numerically investigated the performance of sheet Primitive and Gyroid TPMS geometries. They found that the maximum convection heat transfer coefficient reached 1.400 W/m^{2}K for the Gyroid and 1.413 W/m^{2}K for the Primitive structures.

The aforementioned numerical studies consider work on the unit cell, which is composed of surfaces. There are very few studies that examine the specified geometries as periodic solid geometry instead of sheet unit cells. Also, there is no transient study to examine the real performance of TPMS heat exchangers. This study aims to investigate the flow and heat transfer performance of the Gyroid TPMS structure as a heat exchanger under transient conditions, which is one of the most used TPMS geometries, numerically. Creating the geometry as a solid model with a standard CAD program is very difficult. Therefore, a heat exchanger with a constant porosity value is used to understand the flow and thermal performance. For the stated reasons, this presented study is performed for a single porosity value of 0.6 for a periodic solid geometry. Aluminium, ceramic, and PLA are selected as heat exchanger materials to examine temperature changes in the heat exchanger. Reynolds numbers are chosen at 19.12, 95.61 and 172.09 to investigate the flow regime. Initial air inlet and solid temperatures are assumed to be 298.15 and 278.15 K, respectively, to be consistent with the regenerative heat recovery temperature difference in ventilation standards.

MATERIAL AND METHOD

Mathematical algorithms provide an exact method for Triply Periodic Minimal Surfaces (TPMS), leveraging the definition of minimal surfaces. Various approaches can be employed to design TPMS-based structures, including nodal approximation of the Weierstrass formula, numerical generation methods, and others. However, the simplest and most widely used approach is the level-set equation, which is derived from a sum defined in terms of the Fourier series.

In this study, a cylindrical Gyroid TPMS heat exchanger with 0.6 porosity is built according to Equation 1 by using Mathematica software and exported as .STL file extension. The built geometry is shown in Figure 2. Then, the geometry is imported with ANSYS Space Claim for cleaning, repairing, and fining the surface mesh to obtain the appropriate face size. It ensures that the surfaces generated on the solid model are not too small to produce a poor-quality volume mesh, which can cause convergence problems. The height and diameter of the heat exchanger and the inlet and outlet lengths of the system are chosen as 0.02 m due to reducing computational costs. To ensure that the surface area calculations and resulting heat transfer are not affected by the final surface resolution, the following procedure has been adopted.

$$\cos(x)\sin(y) + \cos(y)\sin(z) + \cos(z)\sin(x) = 0 \qquad (1)$$

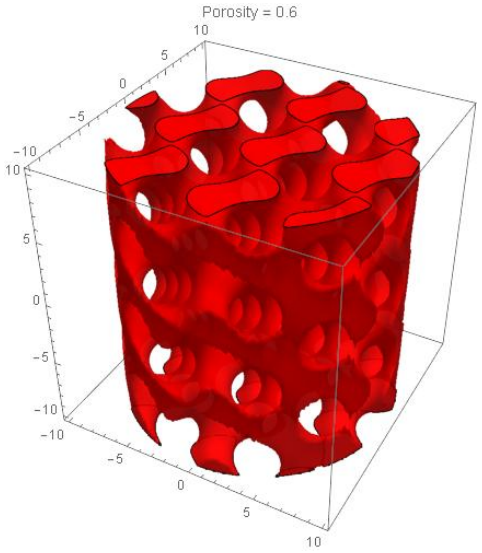

Figure 2. Created geometry by using Mathematica (https://github.com/metudust/RegionTPMS)

The transient 3D numerical model is developed by ANSYS CFX for heat transfer and fluid flow. The geometrical configuration of the computational domain and boundary conditions are shown in Figure 3. Analyses are carried out for Gyroid geometry for varied velocities of 0.1, 0.5 and 0.9 m/s, which correspond to 19.12, 95.61 and 172.09 Reynolds numbers, respectively, at laminar flow. As the boundary condition in the analysis, the outer surfaces of the fluid domain and the solid domain are defined as the walls. The inlet temperature of the fluid to the system is assumed to be 298.15 K, and the initial temperature of the heat exchanger is assumed to be 278.15 K. When choosing these temperatures, the change in the heat capacity of a certain mass over time is considered. Here, indoor, and outdoor temperatures used in ventilation systems are taken as the basis. It is envisaged to be used effectively in heat processes such as heat recovery. Aluminium, ceramic, and PLA are

chosen as heat exchanger materials to compare the differences in thermal properties. The thermophysical properties of the materials are given in Table 1. The thermophysical properties of air at 25 °C are used for the fluid. Natural convection effects have been neglected.

Table 1. Thermophysical properties of heat exchanger materials

Material	k (W/mK)	c_p (J/kgK)	ρ (kg/m³)	α (m²/s)	ρ^*c_p (J/m³K)
Aluminum	237.0	903.0	2700.0	9.71E-05	2.44E+06
Ceramic	1.50	1050.0	2400.0	5.95E-07	2.52E+06
PLA	0.13	1800.0	1300.0	5.58E-08	2.34E+06

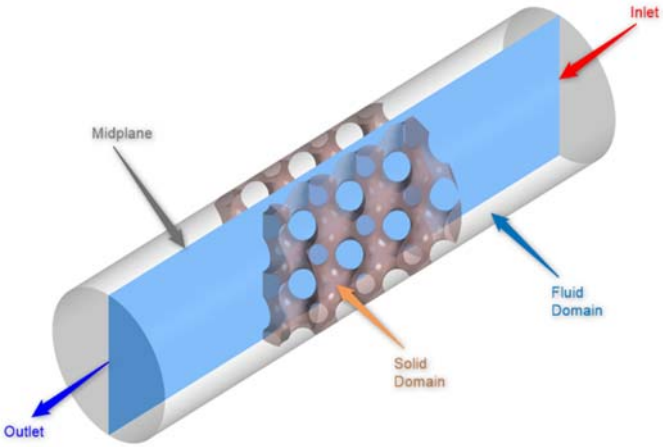

Figure 3. Geometrical configuration of the computational domain and boundary conditions

The Navier-Stokes equations are shown in Equations 2 and 3, respectively. The Shear Stress Transport (SST) turbulence model is used to understand the developed vortexes along the heat exchanger. SST model is prepared by Menter for some missing points of k- ω model. Menter improved the spurious free-stream sensitivity of k- ω model. Two region formularization which utilize k- ω model close wall, k- ε is used for the other part of flow are also improved (Sundén and Faghri, 2005). A high-resolution scheme is used to solve advection terms. For the transient scheme Second Order Backward Euler is used. Convergence criteria are set to 10−6 for all the governing equations.

$$\frac{\partial \rho}{\partial t} + \vec{\nabla}.\left(\rho \vec{V}\right) = 0 \tag{2}$$

$$\rho \frac{\partial V}{\partial t} = -\vec{\nabla}P + \rho \vec{g} + \mu \nabla^2 \vec{V} \tag{3}$$

Mesh independency analysis is conducted for four different mesh element numbers (M1 = 2371748, M2 = 3557621, M3 = 5352423 and M4 = 8884799). Heat rate values, which are critical parameters for the comparison of numerical data, are calculated using M1, M2, M3, and M4 to evaluate mesh independence. According to Figure 4, all meshes are matched up with each other. To evaluate temperature and velocity distributions at higher resolution with reduced computational costs, M2 is chosen. In here, fluid -solid interface element size 0.15 mm, fluid body element size 0.3 mm, solid-fluid interface 0.4 mm, solid body element size. It is determined as 0.8 mm. In places where the element size is small, more frequent mesh is generated. This allows the areas with frequent mesh to be analysed better. The grid quality is ensured with Skewness to be less than 0.8 for all meshes.

Time-step independency is also carried out for 0.05, 0.1, 0.2, 0.4 and 0.5 s. Figure 5 shows that 0.2 s is suitable for obtaining an accurate solution due to the occurring deviation for the first 5 s at 0.4 and 0.5 s time steps. The variation of the total number mesh and/or time step size do not cause any remarkable changes in the time-dependent variation of the heat rate. The maximum deviation between the M1 and the M4 mesh is found to be less than 0.1%. Besides, regarding the time-step size, the maximum difference is obtained as 0.1%. Consequently, the preliminary survey ensures that the results are independent of the mesh number and the time-step size.

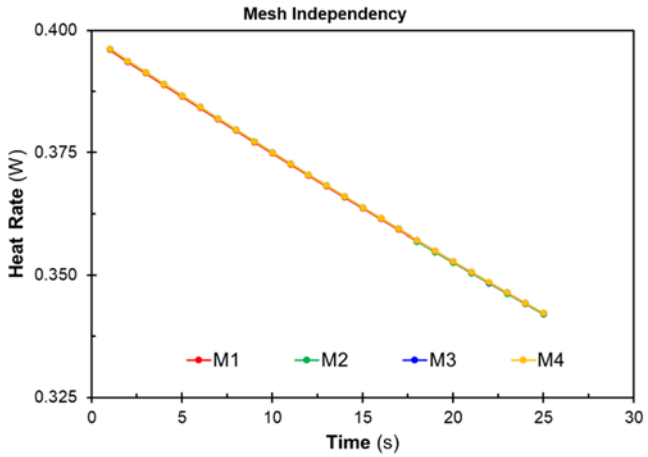

Figure 4. Mesh independency analysis.

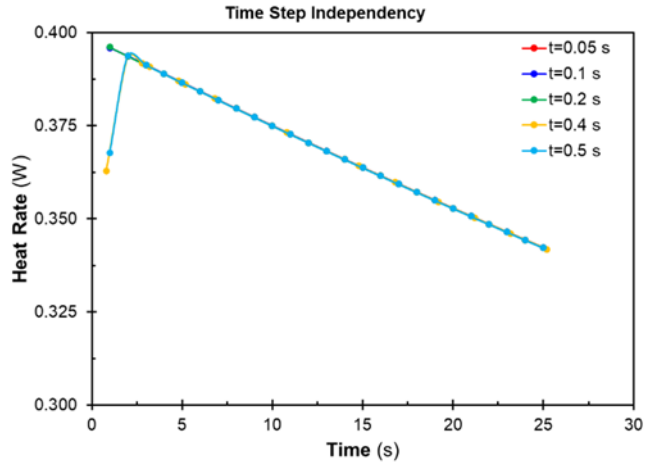

Figure 5. Time step independency

The Reynolds number, *Re,* of the gyroid structure is reported as a hydraulic property which is defined as:

$$Re = \frac{\rho V d_h}{\mu} \tag{4}$$

ρ is the density of the fluid, V is the velocity, d_h is the hydraulic diameter, and μ is the fluid's viscosity. d_h is defined as $4V/A_s$ where V is the domain volume, and A_s is the wetted surface area of the TPMS [6].

The average Nusselt number is defined below:

$$Nu = \frac{\bar{h} d_h}{k} \tag{5}$$

In here, $\bar{h}$ is the average heat transfer coefficient and k is thermal conductivity of the fluid. The averaged heat transfer coefficient, $\bar{h}$ is obtained from analysis results.

Bulk temperature has been calculated with the following equation:

$$T_{bulk} = T_s - (^{T_{inlet} + T_{outlet}}/_{2}) \quad (6)$$

Here, Ts is the surface temperature of the heat exchanger interface, which is conducted with fluid. T_{inlet} and T_{outlet} are the fluid inlet and outlet temperatures, respectively.

The fanning friction coefficient f is expressed as follows:

$$f = \frac{\Delta P d_h}{2\rho V^2 L} \quad (7)$$

where ΔP is the pressure drop; L is the length of the heat exchanger. ΔP was also obtained from analysis results for all velocities.

VALIDATION

Validation of the system was done by Rathore et al. (2023) is carried out according to the pressure drop values per unit length. There are several methods to obtain the pressure drop of porous media and TPMS geometries. One of these methods is presented by Fu et al. (2019), who investigated hydrodynamic and mass transfer performances for Diamond, Gyroid and Primitive TPMS geometries. The following equation is used to calculate the particle or pore diameter (d_p):

$$d_p = \frac{6(1-\varepsilon)}{a_p} \quad (8)$$

Here, ε represents the porosity or void ratio value. a_p is the specific area (m^2/m^3). The rearranged Re number is as follows:

$$Re = \frac{\rho_G V_G d_p}{(1-\varepsilon)\mu_G} = \frac{3}{2}\frac{\rho_G V_G d_{hf}}{\varepsilon \mu_G} \quad (9)$$

Also, d_{hf} means the hydraulic diameter.

$$d_{hf} = \frac{4\varepsilon}{a_p} \quad (10)$$

It is stated that the Re number would be in the range of 0-2500, and the fluid velocity would be in the range of 0-3.5 m/s (Fu et al., 2019). The pressure drop for unit length is calculated by Equation 11:

$$\frac{\Delta p}{\Delta L} = \psi \frac{1-\varepsilon}{\varepsilon}\frac{F_V{}^2}{d_p} \quad (11)$$

$$\psi = \frac{150}{Re} + 1.75 \quad (12)$$

$$F_V = \mu_G \sqrt{\rho_G} \quad (13)$$

The expression ψ is a resistance coefficient that comes from the Ergun equation (Equation 12). $F_V{}^2$ represents the amount of pressure exerted by the fluid (Equation 13).

The present results as shown in Figure 6 match perfectly and therefore indicate the accuracy of the present numerical model.

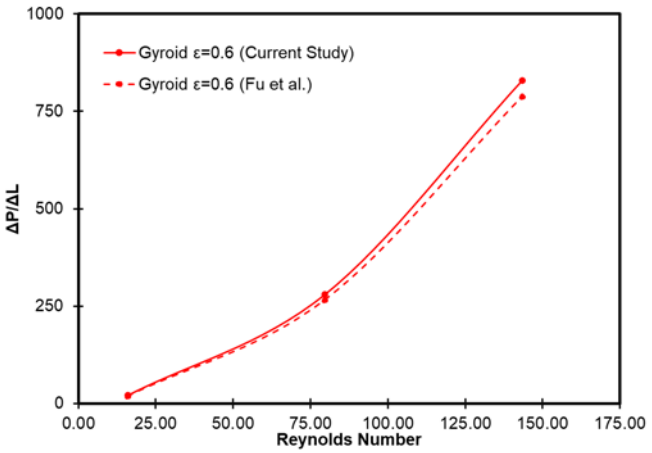

Figure 6. Variation in pressure drop per unit length for the validation study

RESULTS AND DISCUSSIONS

The transient 3D numerical model is developed by ANSYS CFX for heat transfer and fluid flow. Analyses are carried out for gyroid geometry for varied velocities of 0.1, 0.5 and 0.9 m/s and these values correspond to 19.12, 95.61 and 172.09 Reynolds numbers, respectively. All velocities are corresponded to laminar flow. As the boundary conditions, the outer surfaces of both domains are defined as adiabatic. The inlet temperature of the fluid to the system is assumed to be 298.15 K, and the initial temperature of the heat exchanger is assumed to be 278.15 K. Boundary conditions are shown in Figure 3. Also, the midplane is shown to provide a better understanding of the results. Transient analyses are carried out in 0.2 s time steps for a total of 25 s. Aluminium, ceramic and PLA are chosen as heat exchanger materials to compare the difference of thermal properties.

Figure 7. shows the comparison of the friction factor varying Reynolds numbers. The friction factor decreases with increasing Reynolds numbers. These results are similar to an experimental study by Genc et al. (2022).

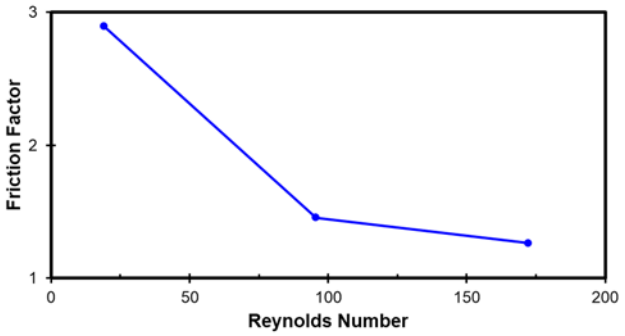

Figure 7. Friction factor against Reynolds number

Figure 8 shows velocity streamlines of 19.12, 95.61 and 172.09 Reynolds numbers for ceramic heat exchanger. While no obvious vortex formation is seen in Figure 7 (a), it begins to form in (b) and becomes most obvious in (c). This shows that as the velocity increases, the vortex formation in the exchanger increases. For a Reynolds number of 19.12, the flow passes through the exchanger at the same velocity, and for a Reynolds number of 95.61, it reaches 2.5 m/s in the exchanger. For the Reynolds number of 172.09, it reaches its highest value as 5 m/s. Similar results can be seen in Figure 8.

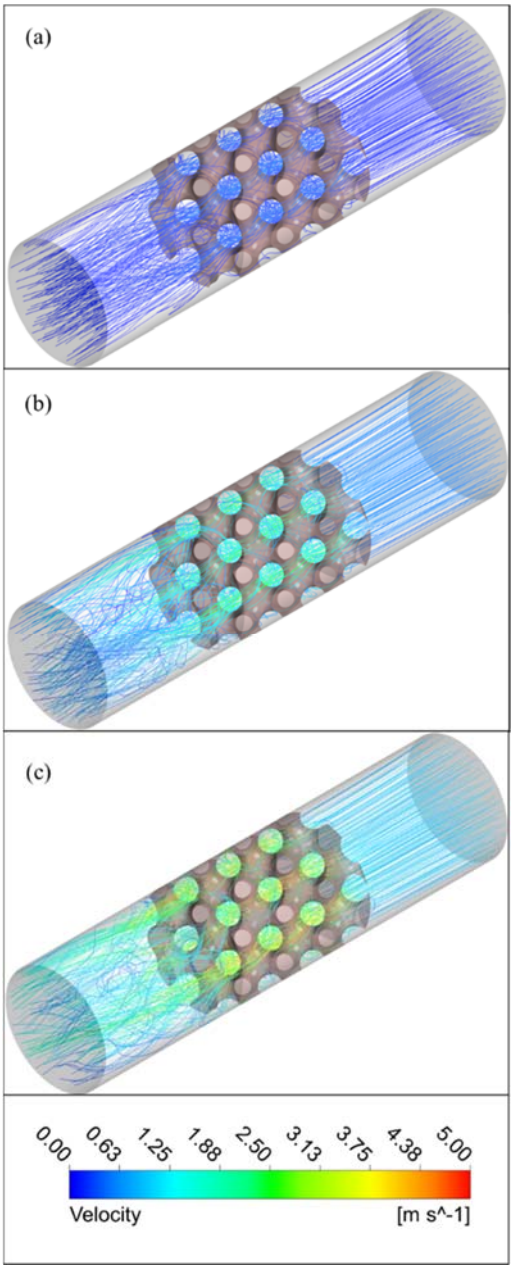

Figure 8. Velocity streamlines for (a) Re=19.12, (b) Re=95.61 and (c) Re=172.09 at 25 s.

Velocity streamlines are also shown in Figure 9 using the system's midplane. It is clear that vortices increase with increasing fluid inlet velocity. Vortices become more evident, especially after the fluid leaves the heat exchanger. This shows that after the fluid accelerates in the exchanger, a vortex forms right at the exchanger's outlet.

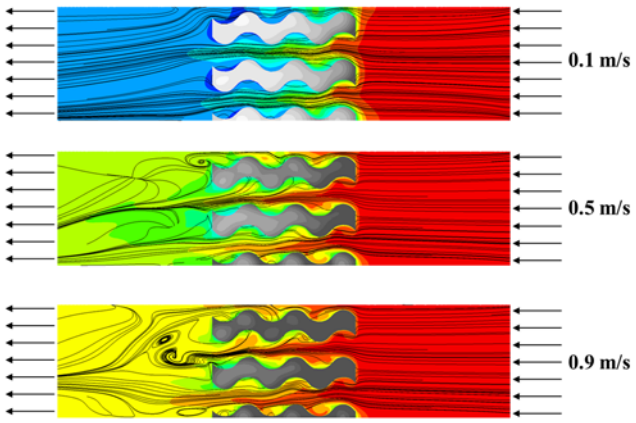

Figure 9. Velocity streamlines for all Reynolds numbers at 25 s.

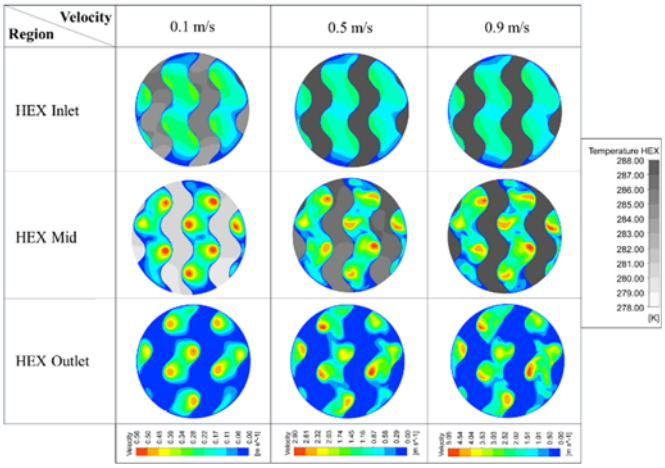

Figure 10. Velocity contours for HEX inlet, mid and outlet planes of ceramic heat exchanger at 25 s.

Figure 10 shows the velocity and temperature contours at the ceramic heat exchanger's HEX inlet, middle and outlet planes. The reason for choosing a ceramic heat exchanger is to achieve higher efficiency in terms of heat transfer. Here, while no significant change is observed for all velocities in the inlet section of the heat exchanger, the velocity increases significantly in the mid-plane and outlet plane, reaching approximately 3 m/s for Re = 95.61 and 5 m/s for Re = 172.09. It is seen that vortex formation begins at the outlet plane for Re = 95.61, and it becomes quite evident for Re = 172.09.

The Nu number against the Re number is shown in Figure 11 for all heat exchanger materials. The Nu number increases with increasing Re number for all. Here, it can be seen that the ceramic has the highest Nu number. As a result of the analysis, the material with the highest average convection coefficient was ceramic. Despite the thermal conductivity of the ceramic material, which is quite lower than the aluminium material, it provides a higher heat transfer rate with its high specific heat capacity and density multiplication (Table 1), that is, volume-specific heat capacity. According to the results, at the highest Re number, it provided approximately 6% better heat transfer than the aluminium heat exchanger.

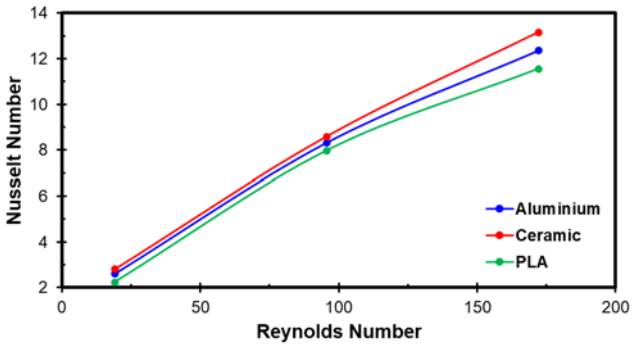

Figure 11. Nu number against Re number

Temperature contours for both solid and fluid domains are shown in Figure 12. There is no significant change in temperature distribution for the aluminium heat exchanger, while the temperature gradients in the ceramic and PLA heat exchanger are more pronounced. The reason for this was the thermal diffusivity. The fact that the ceramic material had a lower thermal diffusivity value ensures that it did not quickly remove the heat from its body (Table 1). At high velocities, the heat capacity of the ceramic heat exchanger decreases. This prevents temperature

distribution within the heat exchanger. However, for PLA heat exchangers, temperature distribution can also be seen at higher velocities. This can be explained by the higher specific heat capacity of PLA material (Table 1). At the highest Reynolds number (172.09), temperatures of 285 K can be observed in the ceramic heat exchanger, while the aluminium heat exchanger reaches 288 K. This value drops to 283 K in the PLA heat exchanger. This is due to its low thermal conductivity and high heat capacity of PLA.

Considering the fluid temperatures, at Re = 19.12, the temperature around the heat exchanger drops to 278 K for ceramic and PLA materials, while it is in the range of 280 - 282 K for the aluminium heat exchanger. While the fluid temperature drops to 286 K for PLA and ceramic materials, it is around 290 K for aluminium materials. In addition to that, at Re = 172.09, as the fluid passes quickly around the exchanger, the temperature generally drops to 292 K.

CONCLUSION

This study aims to numerically investigate the flow and heat transfer performance of the Gyroid structure as a heat exchanger under transient conditions, which is one of the most used TPMS geometries. Creating the geometry as a solid model with a standard CAD program is very difficult. Therefore, a heat exchanger with a porosity value of 0.6 was built to understand flow and thermal performance. For the stated reasons, this presented study was performed for a single porosity value (0.6) for a periodic solid geometry. Aluminium, ceramic, and PLA were selected as the heat exchanger material to examine the temperature change in the heat exchanger. Reynolds numbers are chosen at 19.12, 95.61 and 172.09 to investigate the flow regime. Initial air inlet and solid temperatures were assumed to be 298.15 and 278.15 K, respectively, to be consistent with the regenerative heat recovery temperature difference in ventilation standards.

According to the results:

The velocity increases, the vortex formation in the exchanger increases. For a Reynolds number of 19.12, the flow passes through the exchanger at the same velocity, and for a Reynolds number of 95.61, it reaches 2.5 m/s in the exchanger. For the Reynolds number of 172.09, it reaches its highest value as 5 m/s.

Ceramic material has the highest Nu number. As a result of the analysis, the material with the highest average convection coefficient was ceramic. Despite the thermal conductivity of the ceramic material, which is quite lower than the aluminium material, it provides a higher heat transfer rate with its high specific heat capacity and density multiplication, that is, volume-specific heat capacity and also low thermal diffusivity. According to the results, at the highest Re number, it provided approximately 6% better heat transfer than the aluminium heat exchanger.

While no specific change is observed in the temperature distribution in the aluminium heat exchanger, the temperature gradients are more pronounced in the ceramic and PLA heat exchangers. This is due to thermal diffusivity. The lower thermal diffusivity value of the ceramic and PLA materials ensure that the heat does not quickly dissipate from its body.

Even at low Re numbers, Gyroid geometry creates vortex which causes turbulence in the flow, thus providing high heat transfer. This shows that Gyroid TPMS structures can be used in heat transfer applications.

As future works:

Heat exchangers which have different porosities (0.5, 0.7, 0.8 etc.) and geometries (diamond, primitive) will be built to understand the effect of geometry and porosity.

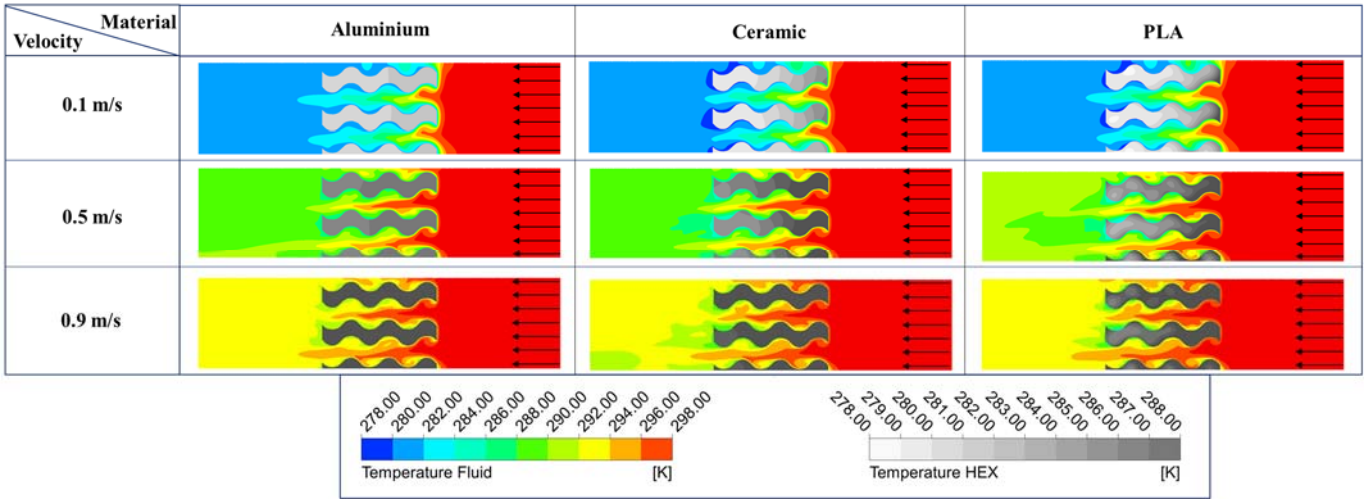

Figure 12. Temperature contours for all heat exchanger materials at 0.1, 0.5 and 0.9 m/s at 25s

REFERENCES

Alteneiji, M., Ali, M. I. H., Khan, K. A., & Al-Rub, R. K. A. Heat transfer effectiveness characteristics maps for additively manufactured TPMS compact heat exchangers, Energy Storage and Saving, Volume 1, Issue 3, 2022.

Barakat, A., & Sun, B. (2024). Enhanced convective heat transfer in new triply periodic minimal surface structures: Numerical and experimental investigation. International Journal of Heat and Mass Transfer, 227, 125538.

Dharmalingam, L.K.; Aute, V.; Ling, J. Review of Triply Periodic Minimal Surface (TPMS) based Heat Exchanger

Designs. In Proceedings of the International Refrigeration and Air Conditioning Conference at Purdue, West Lafayette, IN, USA, 10–14 July 2022.

Femmer, T., Kuehne, A. J., & Wessling, M. (2015). Estimation of the structure dependent performance of 3-D rapid prototyped membranes. Chemical Engineering Journal, 273, 438-445.

Fu, Y., Bao, J., Wang, C., Singh, R. K., Xu, Z., &Panagakos, G. (2019). CFD Study of Countercurrent Flow in Triply Periodic Minimal Surfaces withCO2BOL Solvent (No. PNNL-29590). Pacific Northwest National Lab. (PNNL), Richland, WA (United States).

Genç, A.M.; Vatansever, C.; Koçak, M.; Karadeniz, Z.H. Investigation of Additively Manufactured Triply Periodic Minimal Surfaces as an Air-to-Air Heat Exchanger. In Proceedings of the REHVA 14th HVACWord Congress, Rotterdam, The Netherlands, 22–25 May 2022.

https://github.com/metudust/RegionTPMS

Iyer, J., Moore, T., Nguyen, D., Roy, P., & Stolaroff, J. (2022). Heat transfer and pressure drop characteristics of heat exchangers based on triply periodic minimal and periodic nodal surfaces. Applied Thermal Engineering, 209, 118192.

Kaur, I., & Singh, P. (2021). Flow and thermal transport characteristics of Triply-Periodic Minimal Surface (TPMS)-based gyroid and Schwarz-P cellular materials. Numerical Heat Transfer, Part A: Applications, 79(8), 553-569.

Neovius E.R., Bestimmung Zweier Spezieller Periodischer Minimalflachen, Akad. Abhandlungen, Helsinki, Finland, 1883.

Peng, H., Gao, F., & Hu, W. (2019). Design, modeling and characterization on triply periodic minimal surface heat exchangers with additive manufacturing.

Qian, C., Wang, J., Zhong, H., Qiu, X., Yu, B., Shi, J., & Chen, J. (2024). Experimental investigation on heat transfer characteristics of copper heat exchangers based on triply periodic minimal surfaces (TPMS). International Communications in Heat and Mass Transfer, 152, 107292.

Rathore, S. S., Mehta, B., Kumar, P., & Asfer, M. (2023). Flow characterization in triply periodic minimal surface (TPMS)-based porous geometries: Part 1—Hydrodynamics. Transport in Porous Media, 146(3), 669-701.

Reynolds, B. W., Fee, C. J., Morison, K. R., & Holland, D. J. (2023). Characterisation of heat transfer within 3D printed TPMS heat exchangers. International Journal of Heat and Mass Transfer, 212, 124264.

Reynolds, B.W. Simulation of Flow and Heat Transfer in 3D Printable Triply Periodic Minimal Surface Heat Exchangers; University of Canterbury: Christchurch, New Zealand, 2020.

Schoen A. H., Infinite periyodik minimal surfaces without selfintersections, NASA Technical Note No. D-5541, NASA, 1970.

Schwarz H.A., Ueber ein Modell eines Minimalflachenst€uckes, welches langs seiner Begrenzung vier gegebene Ebenen rechtwinklig trifft. In: Gesammelte Mathematische Abhandlungen, Springer, Berlin, Heidelberg, pp. 149–150, 1890.

Sundén, B., & Faghri, M. (Eds.). (2005). Modelling and Simulation of Turbulent Heat Transfer (Vol. 15). WIT press.

Tang, W., Zhou, H., Zeng, Y., Yan, M., Jiang, C., Yang, P., ... & Zhao, Y. (2023). Analysis on the convective heat transfer process and performance evaluation of Triply Periodic Minimal Surface (TPMS) based on Diamond, Gyroid and Iwp. International Journal of Heat and Mass Transfer, 201, 123642.

Xu, H. J., Gong, L., Zhao, C. Y., Yang, Y. H., & Xu, Z. G. (2015). Analytical considerations of local thermal non-equilibrium conditions for thermal transport in metal foams. International Journal of Thermal Sciences, 95, 73-87.